Comparison of CT Methods for Determining the Fat Content of the Liver

Yoshihisa Kodama[1]
Chaan S. Ng[1]
Tsung T. Wu[2]
Gregory D. Ayers[3]
Steven A. Curley[4]
Eddie K. Abdalla[4]
Jean Nicolas Vauthey[4]
Chusilp Charnsangavej[1]

OBJECTIVE. The purpose of this study was to assess which of a number of methods of measuring attenuation on CT scans is best for prediction of hepatic fat content.

MATERIALS AND METHODS. This retrospective study was approved by our institutional review board. Consecutively registered patients who underwent liver resection for metastatic disease formed the study group. Attenuation measurements were obtained from 12 regions of interest in the liver and three in the spleen on both unenhanced and portal phase contrast-enhanced preoperative hepatic CT images. Hepatic attenuation measurements were analyzed both with and without normalization with the spleen. Normalization included both differences and ratios between hepatic and splenic attenuation values. Pathologic fat content was graded semiquantitatively as a percentage of the nonneoplastic liver parenchyma of the resected specimen. Average attenuation values of the liver were compared with pathologic fat content, as were the differences and ratios between hepatic and splenic attenuation values. Linear regression analysis was conducted on a log-log scale.

RESULTS. Data on 88 patients were analyzed. On unenhanced and contrast-enhanced CT images, all associations between pathologic fat content and attenuation measurements were significant ($p < 0.0001$). All series of R^2 values for unenhanced CT scans were much higher than those for contrast-enhanced CT scans. The R^2 values of liver-only measurement were higher than those of hepatic values normalized with splenic values on both unenhanced (0.646–0.649 > 0.523, 0.565) and contrast-enhanced (0.516 > 0.242, 0.344) CT.

CONCLUSION. Measurement of attenuation of liver only on unenhanced CT scans is best for prediction of pathologic fat content.

Keywords: CT, fat measurement, liver disease

DOI:10.2214/AJR.06.0992

Received July 28, 2006; accepted after revision October 31, 2006.

Presented at the 2006 annual meeting of the American Roentgen Ray Society, Vancouver, BC, Canada.

[1]Department of Diagnostic Radiology, The University of Texas M. D. Anderson Cancer Center, 1515 Holcombe Blvd., Box 368, Houston TX 77030. Address correspondence to C. S. Ng (cng@di.mdacc.tmc.edu).

[2]Department of Pathology, The University of Texas M. D. Anderson Cancer Center, Houston TX.

[3]Department of Biostatistics and Applied Mathematics, University of Texas M. D. Anderson Cancer Center, Houston TX.

[4]Department of Surgical Oncology, The University of Texas M. D. Anderson Cancer Center, Houston TX.

AJR 2007; 188:1307–1312

0361–803X/07/1885–1307

Hepatic steatosis, or fatty liver, is associated with obesity, alcohol consumption, parenteral nutrition, and chemotherapy [1]. It is not a rare condition and generally causes no symptoms. In one study [2], fatty liver was found in 24% of histologic evaluations performed after traffic casualties. Nonalcoholic fatty liver disease defines a spectrum of changes in the liver associated with fat accumulation within the hepatocytes, and that spectrum encompasses both steatosis and steatohepatitis [3]. Nonalcoholic fatty liver disease has been suggested to be the most common form of chronic liver disease in adults, with an estimated prevalence of 3–29% [4, 5]. It has been suggested that nonalcoholic steatohepatitis be considered a progressive form of nonalcoholic fatty liver disease that not only significantly increases the risk of mortality after liver resection [6] but also increases the risk of development of cirrhosis and hepatocellular carcinoma [7–9]. The degree of steatosis that increases the morbidity rate after hepatic resection has been reported by several authors [1, 10, 11] to be 30%. It has also been reported that each 1% increase in hepatic fat content, either microvesicular or macrovesicular, decreases the functional mass of a donor liver 1% [12]. In a recent study [6], steatohepatitis was associated with a greater postoperative mortality than steatosis. The definition of steatohepatitis, based on nonalcoholic fatty liver disease activity score [13], includes a cutoff of 33% for steatosis, corresponding to two points of the score. When the degree of hepatic steatosis becomes significant, the difficulty and risk associated with major hepatic resection increase, and function of hepatic grafts from living donors is impaired [14, 15]. Thus hepatic fat content becomes an important factor to be considered before liver resection.

Histologic examination is accurate in detection of hepatic fat content, but it is invasive and time consuming, and sampling errors can

occur. Noninvasive methods for diagnosing fatty liver include sonography, MRI, and CT. Among these methods, sonography is the easiest, but it is only a qualitative assessment of the fatty liver. MRI is probably the best method for detecting a small amount of fatty infiltration, but it is relatively expensive [16]. CT is the most widely accepted first imaging technique for staging liver metastasis [17].

CT depicts fatty infiltration of the liver as a decrease in attenuation [14, 18–30]. The degree of decrease in CT attenuation has been shown to be related to the degree of fatty infiltration of the liver [18, 22–24]. One issue is that there are several methods for determining the appropriate CT values. These methods include measurement of hepatic attenuation only [18] and normalization of hepatic attenuation with splenic attenuation, such as measurement of the difference in attenuation between liver and spleen [19–21] and calculation of the ratio of these values [22]. To our knowledge, the methods have not been compared. The purpose of this retrospective analysis was to assess which method of measuring attenuation on CT scans is best for prediction of hepatic fat content.

Materials and Methods

Patient Selection

We retrospectively reviewed the database of all patients who had undergone liver resection for metastatic disease at our institution from May 2002 through February 2004. One inclusion criterion was that both unenhanced images and images from the portal venous phase of contrast-enhanced CT (i.e., 60 seconds after injection of contrast material) had been obtained before liver resection. Patients were excluded if pathologic findings had not been reviewed for assessment of the fat content of the liver or if the interval between preoperative CT and resection had been greater than 6 weeks. This retrospective study was approved by our institutional review board.

Multiphasic (triphasic or biphasic) contrast-enhanced and unenhanced CT scans of the liver were evaluated for all patients included in the study. Triphasic studies consisted of the early hepatic arterial, late hepatic arterial, and portal venous phases of contrast enhancement 20, 40, and 60 seconds after administration of contrast medium. An IV injection of 150 mL of nonionic iodinated contrast material (Optiray, Mallinckrodt) was administered at a concentration of 320 mg I/mL and a rate of 5 mL/s. CT was performed at 120 kVp, 240–340 mAs, 5-mm collimation, pitch of 1.5, and 5-mm reconstruction interval. Biphasic studies consisted of late hepatic arterial and portal venous phase images obtained approximately 40 and 60 seconds after IV injection of 150 mL of nonionic iodinated contrast material at a concentration of 320 mg I/mL and a rate of 3 mL/s. CT was performed at 120 kVp, 240–340 mAs, 7.5-mm collimation, pitch of 0.75, and 7.5-mm reconstruction interval. Biphasic studies were generated in cases in which patients had undergone combined chest and abdominal CT. The images from the portal venous phase (i.e., 60 seconds after contrast injection) were used as contrast-enhanced images in the analyses. All scans were obtained with 4-MDCT scanners (LightSpeed, GE Healthcare).

Attenuation Measurements

We delineated 12 regions of interest (ROIs) within the liver on the CT scans of each patient and obtained the attenuation measurements for each ROI. One radiologist with 11 years of experience used both unenhanced and contrast-enhanced CT images to delineate the ROIs by selecting three representative levels. The levels contained the confluence of the right hepatic vein (Figs. 1A and 2A), the umbilical portion of the left portal vein (Figs. 1B and 2B), and the posterior branch of the right portal vein (Figs. 1C and 2C). At each representative level, the liver was apportioned into four sectors (right posterior, right anterior, left medial, and left lateral). These sectors were defined with a modification of the Couinaud [31] segmentation system. The right posterior sector included segments VI and VII, the right anterior sector included segments V and VIII, the left medial sector included segment IV, and the left lateral sector included segments II and III. One ROI randomly drawn inside each sector, avoiding the large vessels and any focal lesions, was considered representative of the sector. Each ROI measured 1.0 ± 0.1 cm^2. We also drew one ROI inside the spleen in each representative slice (Fig. 2).

Pathologic Fat Content

Pathologic fat content was measured in representative H and E slides from the resected liver specimen. In each case, one pathologist with 5 years of experience who had expertise in gastrointestinal and hepatic pathology graded the degree of steatosis using slides of tissue specimens from nonneoplastic liver parenchyma at least 2 cm away from the metastatic tumor. The degree of steatosis was graded semiquantitatively as the percentage of liver parenchyma involved by fatty infiltration, estimated to the nearest 5%. When the degree of involvement was less than 5%, it was estimated to the nearest 1%.

Statistical Analysis

For each patient, average attenuation in the ROIs in whole sectors of the liver and that in the resected sectors of the liver was calculated on both unenhanced and contrast-enhanced CT scans. A sector was considered resected only if it actually contained a resected segment. For example, in the case of a patient who had undergone right extended hepatectomy, the right posterior, right anterior, and left medial sectors were defined as resected sectors. The average attenuation of the ROIs in the spleen also was calculated.

We first transformed the value for pathologic fat content to –log[–log (pathologic fat content)]. This is a common transformation for proportions to meet the normality assumptions of the least-squares linear regression model. Because pathologic fat content values less than 1 were undefined in this transformation, such values were imputed with Markov chain Monte Carlo methods (20,000 replicates). Linear regression equations for prediction of the transformed pathologic fat content were estimated from whole-liver attenuation, attenuation of whole liver minus spleen, ratio of whole-liver attenuation to splenic attenuation, attenuation of the resected portion of the liver, attenuation of the resected portion of the liver minus the spleen, and ratio of resected liver attenuation to splenic attenuation. Coefficient of determination (R^2), mean square error of the regression line (S^2), and p values were calculated. In comparisons of regression models, larger R^2 values and smaller S^2 values imply superior predictive ability.

Back-transformed estimates of the predicted pathologic fat content with 90% CIs have a sensible lower bound of zero. Regressions incorporating Markov chain Monte Carlo methods were conducted with R Project software (R Foundation for Statistical Computing) (free software available at: www.r-project.org). Graphs of observed and predicted models with 90% CIs were constructed with S-Plus software (Insightful).

Results

During the study period, 157 patients underwent liver resection for metastatic disease at our institution. Fifty-eight of the patients were excluded from analysis because they did not undergo both unenhanced and contrast-enhanced CT. Eight patients were excluded because pathologic findings were not available, and three were excluded because the interval between preoperative CT and resection was greater than 6 weeks. Thus data on 88 patients formed the basis of this retrospective study. Forty-two of the 88 patients were women. The median age at resection was 58 years (range, 18–81 years), and the mean interval between preoperative CT and resection was 16.4 days (range, 1–36 days). The mean number of hepatic metastatic lesions was 2.6 (range, 1–12 lesions). Multiphasic (59 triphasic, 29 biphasic) contrast-enhanced and unenhanced CT scans of the liver were available for all 88 patients.

Table 1 shows the data (mean ± SD) for all attenuation calculations for both unenhanced and contrast-enhanced CT scans. Table 2

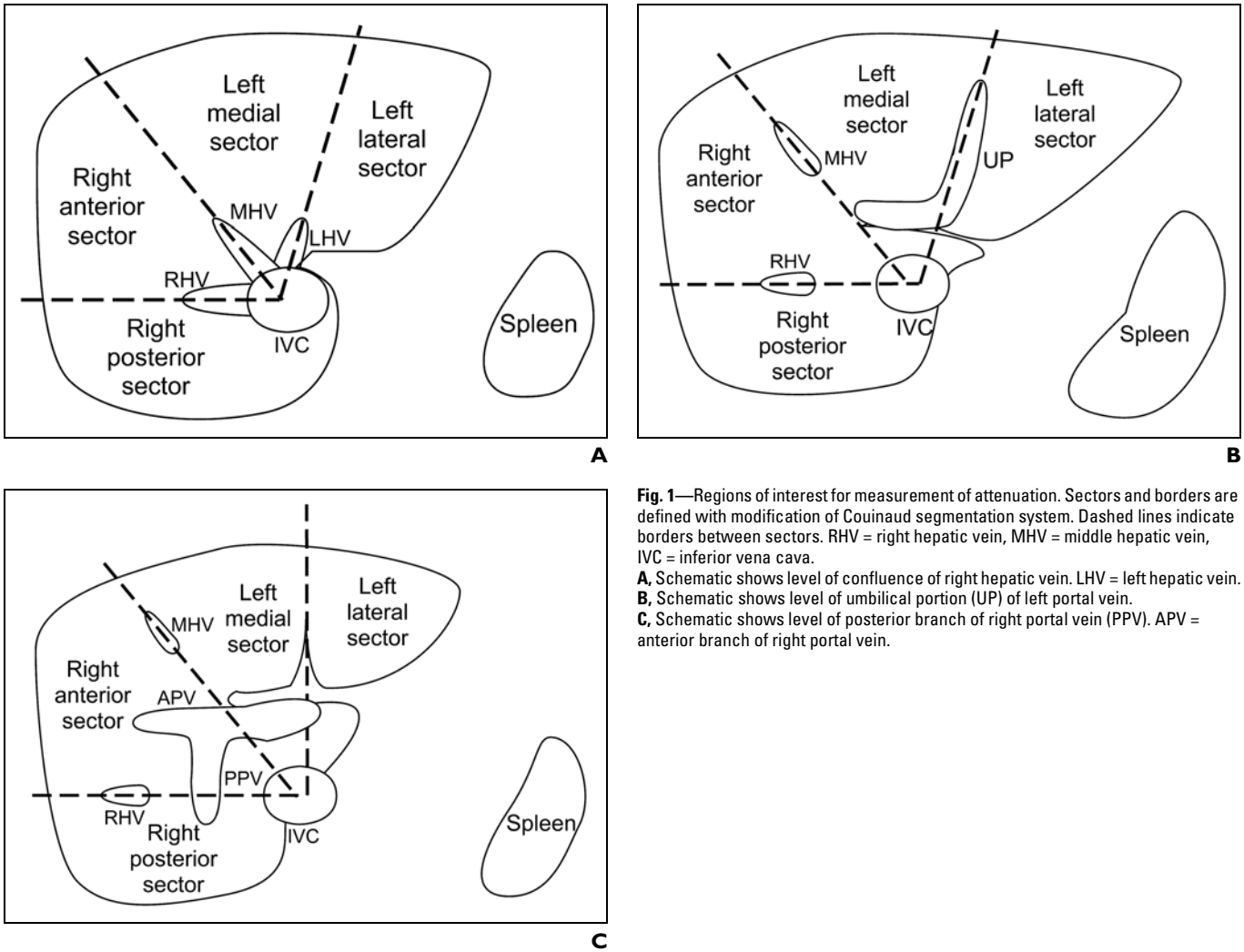

Fig. 1—Regions of interest for measurement of attenuation. Sectors and borders are defined with modification of Couinaud segmentation system. Dashed lines indicate borders between sectors. RHV = right hepatic vein, MHV = middle hepatic vein, IVC = inferior vena cava.
A, Schematic shows level of confluence of right hepatic vein. LHV = left hepatic vein.
B, Schematic shows level of umbilical portion (UP) of left portal vein.
C, Schematic shows level of posterior branch of right portal vein (PPV). APV = anterior branch of right portal vein.

shows the mean (± SD) data for attenuation calculations for unenhanced CT scans categorized by pathologic fat content. Overall, the mean pathologic fat content was 12.9% ± 16.9% (range, 0–70%). This value includes data on the 19 (22%) of the patients in whom no fat was detected in the liver. All regression estimates of the slopes predicting pathologic fat content from attenuation calculations for both unenhanced and contrast-enhanced CT scans were statistically significant at $p < 0.0001$ (Table 3). All series of R^2 values for the unenhanced CT scans were much higher than those for the contrast-enhanced images (Table 3). The difference in R^2 values between whole-liver attenuation and resected-liver attenuation was very small for both unenhanced (0.649 and 0.646) and contrast-enhanced CT images (0.516 and 0.516). The R^2 values for whole-liver attenuation and resected-liver attenuation without comparison with splenic attenuation were higher than the values in which splenic measurements were considered (i.e., whole liver minus spleen, resected liver minus spleen, ratio of whole-liver to splenic attenuation, and ratio of resected-liver to splenic attenuation) on both unenhanced (0.646–0.649 > 0.523–0.565) and contrast-enhanced (0.516 > 0.242–0.344) images (Table 3).

The regression line of pathologic fat content versus unenhanced resected-liver attenuation was pathologic fat content = exp[–exp(–1.915 + 0.051 × resected-liver attenuation)] and is plotted in Figure 3A along with observed pathologic fat content values. On the basis of this regression equation, if the liver attenuation on unenhanced CT scans is 40 H, the predicted hepatic fat content is approximately 30%. Similarly, if the unenhanced CT attenuation is 30 H, the predicted hepatic fat content is approximately 50%. The regression line of pathologic fat content versus contrast-enhanced resected-liver attenuation was pathologic fat content = exp[–exp(–1.781 + 0.024 × resected-liver attenuation)] and is plotted in Figure 3B along with the observed pathologic fat content values.

Discussion

We found that the best method of predicting pathologic fat content in the liver is simple measurement of liver attenuation on unenhanced CT scans. Previous reports have shown unenhanced CT images to be good for prediction of the degree of fatty infiltration of the liver [18, 22–24]. Ducommun et al. [18] and Kawata et al. [23] found that attenuation of the liver on CT scans accurately reflected pathologic fat content in rabbits. Ricci et al. [22] reported that fat content in the liver, represented by a fat-containing tube model, had a linear correlation with CT attenuation. Wang et al. [24] suggested that dual-energy CT was useful for making a quantitative diagnosis of fatty liver in a rabbit model.

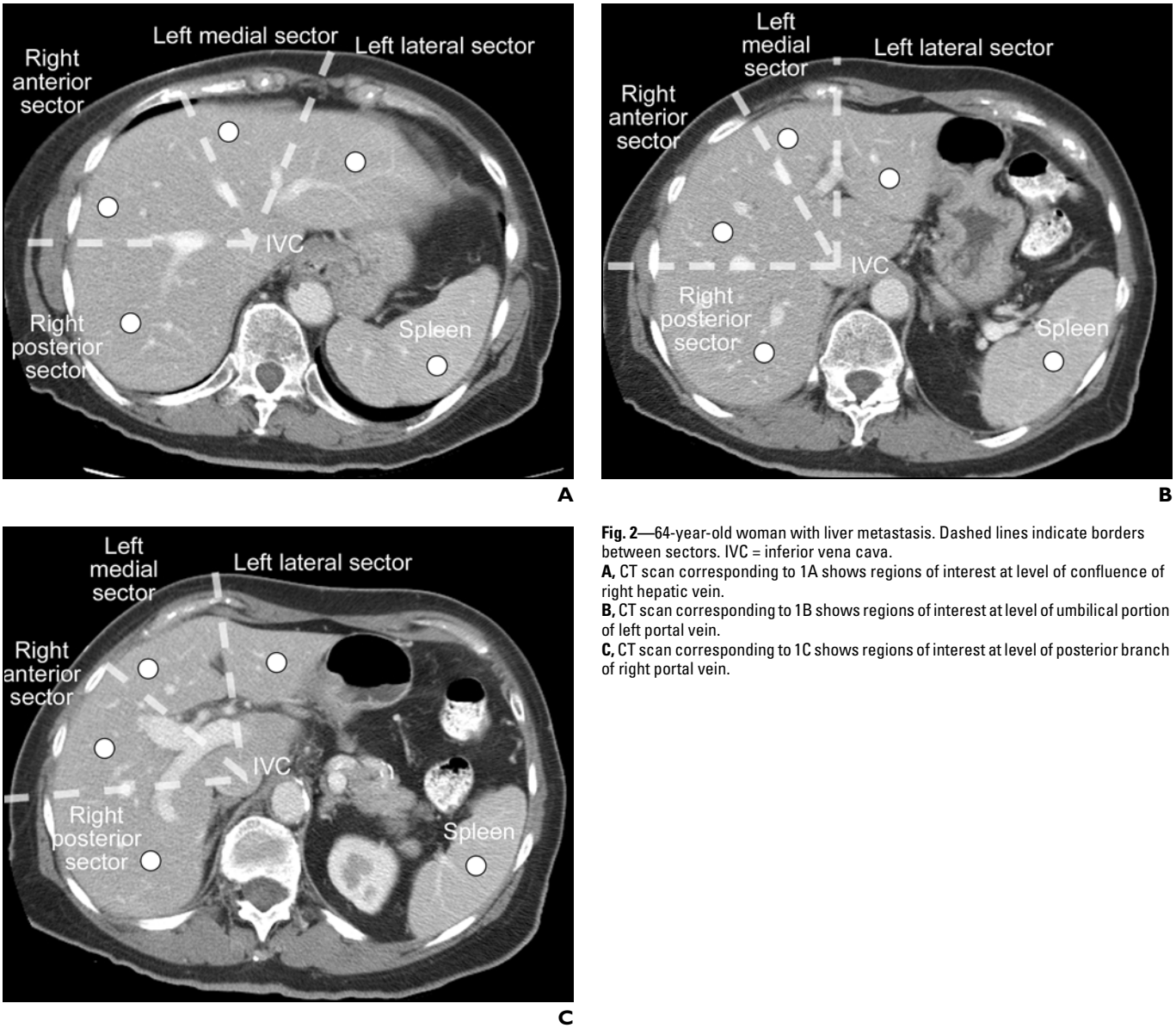

Fig. 2—64-year-old woman with liver metastasis. Dashed lines indicate borders between sectors. IVC = inferior vena cava.
A, CT scan corresponding to 1A shows regions of interest at level of confluence of right hepatic vein.
B, CT scan corresponding to 1B shows regions of interest at level of umbilical portion of left portal vein.
C, CT scan corresponding to 1C shows regions of interest at level of posterior branch of right portal vein.

TABLE 1: Attenuation Values

CT Type	Whole Liver	Resected Portion of Liver	Spleen	Whole Liver Minus Spleen	Resected Portion of Liver Minus Spleen	Ratio Between Whole Liver and Spleen	Ratio Between Resected Liver and Spleen
Unenhanced							
Average attenuation (H)	56.5	56.4	53.0	3.6	3.4	1.07	1.07
SD	11.7	11.7	4.5	11.3	11.3	0.23	0.23
Contrast-enhanced							
Average attenuation (H)	116.0	116.5	132.7	–16.7	–16.2	0.88	0.88
SD	24.0	24.4	22.0	20.6	21.1	0.15	0.15

In our study, all series of R^2 values for the unenhanced CT images were much higher than those for the contrast-enhanced images, indicating that contrast-enhanced CT was not the most suitable method for prediction of hepatic fat content. This finding was similar to those previously reported [20, 21]. On contrast-enhanced CT, attenuation is greatly affected by the concentration of the contrast

TABLE 2: Attenuation Categorized by Pathologic Fat Content on Unenhanced CT

Pathologic Fat Content (%)	No.	Attenuation (H)[a]	
		Whole Liver	Resected Portion of Liver
0	19	64.4 ± 3.1	63.9 ± 3.7
1–25	54	59.1 ± 7.3	59.1 ± 7.1
26–50	11	41.9 ± 6.7	40.8 ± 7.2
> 50	4	25.0 ± 15.5	26.2 ± 14.9

[a]Values are mean ± SD.

medium, which is greatly affected by volume, rate of administration, and circulation of contrast material and the timing of measurements [20]. We used two different injection rate protocols, which likely contributed to the variability. The SD of attenuation in contrast-enhanced series was larger than in unenhanced series. Thus any difference in attenuation due to fat content was masked by the effect of the contrast medium, which resulted in a decrease in prediction power.

The spleen provides a suitable organ to which the liver might potentially be normalized. Overall splenic attenuation is not affected by most diffuse pathologic processes, and the spleen is usually located on the same axial CT slice as the liver, making it easy to measure the attenuation [20]. In our study, we measured attenuation not only of the liver but also of the spleen and analyzed both the differences and the ratios between the hepatic and splenic attenuation values.

In comparisons of attenuation measurements of liver only and of liver normalized with spleen, the R^2 values of liver only were higher than those of liver normalized with spleen. The difference was not small, indicating that attenuation measurement in the spleen did not contribute to the prediction of hepatic fat content. We were somewhat surprised by this result because we were anticipating a normalizing effect with the inclusion of splenic measurement.

The R^2 value of resected-liver attenuation was a bit smaller than that of whole-liver attenuation, although this difference was inconsequential. We expected that the attenuation of the resected portions of the liver would be

TABLE 3: Results of Linear Regression Analysis

Value	Whole Liver	Resected Portion of Liver	Whole Liver Minus Spleen	Resected Portion of Liver Minus Spleen	Ratio Between Whole Liver and Spleen	Ratio Between Resected Portion of Liver and Spleen
Unenhanced CT						
R^2	0.649	0.646	0.565	0.555	0.535	0.523
S^2	0.198	0.200	0.252	0.259	0.270	0.279
Contrast-enhanced CT						
R^2	0.516	0.516	0.251	0.242	0.344	0.331
S^2	0.325	0.329	0.483	0.487	0.411	0.420

Note—All series of comparisons between pathologic fat content and attenuation calculations are $p < 0.0001$. R^2 = coefficient of determination, S^2 = mean square error of regression line.

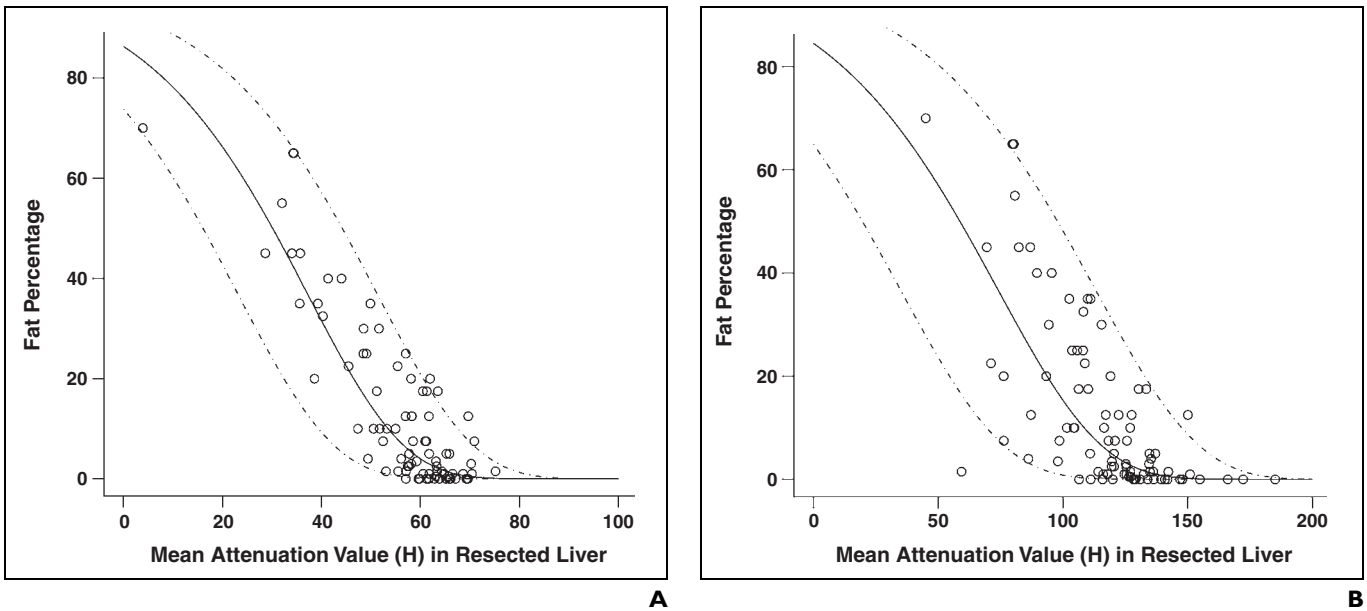

Fig. 3—Fat content versus attenuation.
A, Graph shows results for unenhanced CT images. Solid line indicates predictive equation for pathologic fat content given attenuation of resected portion of liver. Pathologic fat content = exp[–exp(–1.915 + 0.051 × resected-liver attenuation)]. Dashed lines indicate upper and lower 90% bounds of pathologic fat content.
B, Graph shows results for contrast-enhanced CT images. Solid line indicates predictive equation for pathologic fat content given attenuation of resected portion of liver. Pathologic fat content = exp[–exp(–1.781 + 0.024 × resected-liver attenuation)]. Dashed lines indicate upper and lower 90% bounds of pathologic fat content.

more useful than that of whole liver for prediction of fat content, which was obtained from the resected portions of liver. The difference was very small, however, leading us to conclude that there is no difference in predictive capacity between the attenuation of whole liver and that of resected liver segments.

We recognize that this study had limitations. First, the exact sites from which the pathologic sections were obtained for evaluation of pathologic fat content were not precisely defined. Thus we did not undertake location-to-location correlation between the pathologic specimens and the attenuation measurements. Second, liver attenuation is affected not only by fat infiltration but also by other metabolic conditions, such as iron deposition [32] and hepatic edema, as in hepatitis. When fatty infiltration and iron deposition coexist, a change in attenuation of the liver can be masked [15]. Third, focal fatty infiltration sometimes occurs, and in those cases, attenuation of the liver is heterogeneous rather than homogeneous [25, 26]. Because it is difficult to define the degree of heterogenicity, we included all cases, even those with heterogenicity. We measured a large number of ROIs and used the average value for analysis. We believe that this method minimizes the effect of heterogenicity.

Comparison of hepatic attenuation with splenic attenuation is a more complex method than measuring liver attenuation alone. The liver–spleen method requires more time and effort. Because our results showed that splenic measurements did not contribute to accurate prediction of fat content, we consider comparison methods unnecessary. Simple liver attenuation measurement not only saves time and effort but also gives an intelligible and useful result.

It has been suggested [1, 10, 11] that a hepatic fat content greater than 30% increases the risk of morbidity after hepatic resection. For this reason, it also has been suggested [15] that persons with a hepatic fat content greater than 30% should not be liver donors. Results with our regression model indicate that a practical cutoff value for predicting 30% liver fat content may be an attenuation of 40 H on unenhanced CT scans. We conclude that radiologists and clinicians can use liver-only attenuation to easily define the degree of fatty infiltration of the liver.

Acknowledgments

We thank Valen E. Johnson for statistical consultation, Delise H. Herron and Ella F. Anderson for technical assistance, and Karen Phillips and Kathryn Hale for invaluable assistance in preparing the manuscript.

References

1. Kooby DA, Fong Y, Suriawinata A, et al. Impact of steatosis on perioperative outcome following hepatic resection. *J Gastrointest Surg* 2003; 7:1034–1044
2. Hilden M, Christoffersen P, Juhl E, Dalgaard JB. Liver histology in a "normal" population: examinations of 503 consecutive fatal traffic casualties. *Scand J Gastroenterol* 1977; 12:593–597
3. Oliva MR, Mortele KJ, Segatto E, et al. Computed tomography features of nonalcoholic steatohepatitis with histopathologic correlation. *J Comput Assist Tomogr* 2006; 30:37–43
4. Clark JM, Brancati FL, Diehl AM. Nonalcoholic fatty liver disease. *Gastroenterology* 2002; 122:1649–1657
5. Jimba S, Nakagami T, Takahashi M, et al. Prevalence of non-alcoholic fatty liver disease and its association with impaired glucose metabolism in Japanese adults. *Diabet Med* 2005; 22:1141–1145
6. Vauthey JN, Pawlik TM, Ribero D, et al. Chemotherapy regimen predicts steatohepatitis and an increase in 90-day mortality after surgery for hepatic colorectal metastases. *J Clin Oncol* 2006; 24:2065–2072
7. McCullough AJ. Update on nonalcoholic fatty liver disease. *J Clin Gastroenterol* 2002; 34:255–262
8. Regimbeau JM, Colombat M, Mognol P, et al. Obesity and diabetes as a risk factor for hepatocellular carcinoma. *Liver Transpl* 2004; 10:S69–S73
9. Bugianesi E, Leone N, Vanni E, et al. Expanding the natural history of nonalcoholic steatohepatitis: from cryptogenic cirrhosis to hepatocellular carcinoma. *Gastroenterology* 2002; 123:134–140
10. Behrns KE, Tsiotos GG, DeSouza NF, Krishna MK, Ludwig J, Nagorney DM. Hepatic steatosis as a potential risk factor for major hepatic resection. *J Gastrointest Surg* 1998; 2:292–298
11. Belghiti J, Hiramatsu K, Benoist S, Massault P, Sauvanet A, Farges O. Seven hundred forty-seven hepatectomies in the 1990s: an update to evaluate the actual risk of liver resection. *J Am Coll Surg* 2000; 191:38–46
12. Marcos A. Right lobe living donor liver transplantation: a review. *Liver Transpl* 2000; 6:3–20
13. Kleiner DE, Brunt EM, Van NM, et al. Design and validation of a histological scoring system for nonalcoholic fatty liver disease. *Hepatology* 2005; 41:1313–1321
14. Cheng YF, Chen CL, Lai CY, et al. Assessment of donor fatty livers for liver transplantation. *Transplantation* 2001; 71:1221–1225
15. Limanond P, Raman SS, Lassman C, et al. Macrovesicular hepatic steatosis in living related liver donors: correlation between CT and histologic findings. *Radiology* 2004; 230:276–280
16. Levenson H, Greensite F, Hoefs J, et al. Fatty infiltration of the liver: quantification with phase-contrast MR imaging at 1.5 T vs biopsy. *AJR* 1991; 156:307–312
17. Charnsangavej C, Clary B, Fong Y, et al. Selection of patients for resection of hepatic colorectal metastases: expert consensus statement. *Ann Surg Oncol* 2006; 13:1261–1268
18. Ducommun JC, Goldberg HI, Korobkin M, Moss AA, Kressel HY. The relation of liver fat to computed tomography numbers: a preliminary experimental study in rabbits. *Radiology* 1979; 130:511–513
19. Piekarski J, Goldberg HI, Royal SA, Axel L, Moss AA. Difference between liver and spleen CT numbers in the normal adult: its usefulness in predicting the presence of diffuse liver disease. *Radiology* 1980; 137:727–729
20. Johnston RJ, Stamm ER, Lewin JM, Hendrick RE, Archer PG. Diagnosis of fatty infiltration of the liver on contrast enhanced CT: limitations of liver-minus-spleen attenuation difference measurements. *Abdom Imaging* 1998; 23:409–415
21. Jacobs JE, Birnbaum BA, Shapiro MA, et al. Diagnostic criteria for fatty infiltration of the liver on contrast-enhanced helical CT. *AJR* 1998; 171:659–664
22. Ricci C, Longo R, Gioulis E, et al. Noninvasive in vivo quantitative assessment of fat content in human liver. *J Hepatol* 1997; 27:108–113
23. Kawata R, Sakata K, Kunieda T, Saji S, Doi H, Nozawa Y. Quantitative evaluation of fatty liver by computed tomography in rabbits. *AJR* 1984; 142:741–746
24. Wang B, Gao Z, Zou Q, Li L. Quantitative diagnosis of fatty liver with dual-energy CT: an experimental study in rabbits. *Acta Radiol* 2003; 44:92–97
25. Halvorsen RA, Korobkin M, Ram PC, Thompson WM. CT appearance of focal fatty infiltration of the liver. *AJR* 1982; 139:277–281
26. Kammen BF, Pacharn P, Thoeni RF, et al. Focal fatty infiltration of the liver: analysis of prevalence and CT findings in children and young adults. *AJR* 2001; 177:1035–1039
27. Scherer U, Santos M, Lissner J. CT studies of the liver in vitro: a report on 82 cases with pathological correlation. *J Comput Assist Tomogr* 1979; 3:589–595
28. Panicek DM, Giess CS, Schwartz LH. Qualitative assessment of liver for fatty infiltration on contrast-enhanced CT: is muscle a better standard of reference than spleen? *J Comput Assist Tomogr* 1997; 21:699–705
29. Jain KA, McGahan JP. Spectrum of CT and sonographic appearance of fatty infiltration of the liver. *Clin Imaging* 1993; 17:162–168
30. Nomura F, Ohnishi K, Ochiai T, Okuda K. Obesity-related nonalcoholic fatty liver: CT features and follow-up studies after low-calorie diet. *Radiology* 1987; 162:845–847
31. Couinaud C. Liver anatomy: portal (and suprahepatic) or biliary segmentation. *Dig Surg* 1999; 16:459–467
32. Mills SR, Doppman JL, Nienhuis AW. Computed tomography in the diagnosis of disorders of excessive iron storage of the liver. *J Comput Assist Tomogr* 1977; 1:101–104